NEW METHODOLOGY TO DESIGN GROUND COUPLED HEAT PUMP SYSTEMS BASED ON TOTAL COST MINIMIZATION

Félix Robert, Louis Gosselin[1]

Département de génie mécanique, Université Laval, Québec City, Québec, Canada, G1V 0A6

Abstract

This paper introduces a method for designing vertical ground heat exchangers and heat pump systems, by minimizing the total cost of the project. The total cost includes an initial cost composed of drilling, excavation, heat pump and piping network. An operational cost is also included to account for the energy consumed for heating/cooling a building. The procedure allows determining the optimal number of boreholes, their depth and spacing, and the optimal size of the heat pump. The method is tested for different ground conductivity and heat demands. The method can also be used to determine the economical viability of a TRT. For tested cases, results show that the excess cost due to uncertainty on ground thermal conductivity increases with the number of boreholes. Also, a cost sensibility analysis shows that the most influential parameters are the number of boreholes and their depth.

Keywords: ground source heat pump; borefield; optimization; cost; geothermal; thermal conductivity

Nomenclature

A area, m^2

B distance between boreholes, m

C cost, $

c specific heat, J kg^{-1} K^{-1}

D diameter, m

H borehole depth, m

[1] Corresponding Author. Louis.Gosselin@gmc.ulaval.ca, Tel.: +418-656-7829, Fax: +418-656-7415.

j	interest rate, %
k	thermal conductivity, W m^{-1} K^{-1}
L	length, m
$\dot{m}$	mass flow rate, kg s^{-1}
N	number of boreholes in x or y direction
$\Delta P'$	pipe head loss per unit length, Pa m^{-1}
p	percentage of total heat load
Q	thermal energy, kWh
$\dot{Q}$	heat transfer rate, W
q	heat load per length unit, W m^{-1}
R	conduction resistance, K W^{-1}
T	temperature, °C
t	time, h
W	work energy, kWh
$\dot{W}$	work or power, W
X	price, $

Greek Symbols

α	thermal diffusivity, m^2 s^{-1}
μ	viscosity, kg s^{-1} m^{-1}
ρ	density, kg m^{-3}

1. Introduction

Among available options, geothermal energy is known to be a particularly good alternative for heating and cooling buildings, in terms of energy efficiency and environmental impacts [1]. That explains in part why the world's direct utilization of geothermal energy grew up by 43% from 2000 to 2005 [2][3]. In Canada, ground

temperature is relatively cold (around 6°C [4]), and therefore, building heating based on geothermal energy requires a ground coupled heat pump (GCHP) system. Vertical heat exchangers are among the most widely used configurations, but other types of ground heat collector designs can also be considered (e.g., horizontal heat exchangers, open loop systems, etc.).

Although GCHP systems can yield significant and recurrent energy savings compared to "more traditional" heating/cooling systems [5], the high investment that they require is one of the main reasons preventing these systems to be more widely used in practice. Therefore, accurate and efficient sizing procedures are particularly important in order to avoid under or over-designs which is accompanied by a reduction of energy savings or by excess initial costs. On the other hand, present design and sizing strategies rely mostly on approximate "rules of thumbs" (e.g., specified number of meters of borehole per kW of heating/cooling) or on achieving an acceptable level of performance based on a worst case scenario. In particular, in the latter category, ASHRAE's proposed method [6] is among the most widely used. Given the heating/cooling load assumed by the ground, the procedure essentially estimates the required length of borehole in order to satisfy the heating/cooling needs after ten years, in the peak period. In that procedure, a certain grid of borehole is assumed by the designer, and a penalty temperature is considered in order to account for borehole-to-borehole thermal interactions in that configuration [7].

Despite their valuable and practical usefulness, current design methods for geothermal systems also have limitations. For example, the designer has to decide or impose a priori the proportion of the building heating and cooling needs that will rely on geothermal energy. Also, and most importantly, there is no guarantee that the final design is the most cost-effective.

Total cost minimization procedures have been developed to design many systems, including different types of heat exchangers, e.g. Refs. [8], [9], [10], and [11]. Overall, this body of work showed that it is possible to determine the 'best' heat exchanger geometrical and operational features to minimize its overall cost, for a given duty. In this paper, we thus propose a new design and sizing method for vertical ground heat exchangers coupled to a heat pump based on total cost minimization.

2. Evaluation of the cost function

In the present section, we explain how the total cost of a ground source heat pump system project was evaluated. Eventually, this global cost will be minimized with respect to a series of design variables in order to determine optimal design features (see Section 4). The total cost of the project is obtained by summing the operating costs with the initial capital invested. Every annual money flux was converted into its present value, in such a way that the total cost could be expressed as:

$$C_{tot} = C_{initial} + \sum_{y=1}^{n} C_{a,y} \left(1+ j\right)^{-y} \quad (1)$$

where n is the number of years of the project, j, the interest rate [%] and $C_{a,1}\ldots C_{a,n}$ are the annual operating cost for years 1 to n. The two next sections explain how the operating and initial costs were calculated.

2.1 Operating cost

The operating cost is mostly governed by the energy consumed by three devices: the heat pump, the heat transfer fluid circulation pump, and the backup heating/cooling system.

The instantaneous power needed by the heat pump depends on its coefficient of performance (COP) as well as on the building heat load that the geothermal system is taking care of. In the present analysis, it is considered that only a ratio p of the building peak load $\dot{Q}_{max}$ is provided by the geothermal system. In other words, the system is sized in such a way that when the instantaneous building heating requirement is larger than $p\dot{Q}_{max}$, a backup system is used to supply the exceeding heating requirement. In the present study, it is supposed that the system operates in a heating dominant environment. Therefore, no backup system for the cooling load was considered (i.e. all cooling is provided by the borefield). The method outlined in this paper could easily be adapted to situations where the cooling load is more important by including the cooling backup cost. Mathematically, the building heating load provided by the geothermal heat pump can be written as:

$$\dot{Q}_{build,HP}(t) = \begin{cases} \dot{Q}_{build}(t) & \left(\dot{Q}_{build}(t) \le p\dot{Q}_{\max}\right) \\ p\dot{Q}_{\max} & \left(\dot{Q}_{build}(t) > p\dot{Q}_{\max}\right) \end{cases} \quad (2)$$

Then, the instantaneous power requirement is:

$$\dot{W}_{HP}(t) = \dot{Q}_{build,HP}(t) / COP(t) \quad (3)$$

Note that in current practices, p is usually assumed by the designer, whereas in the present procedure, it will be optimized in order to minimize total cost.

The power required for the backup system is determined by subtracting the heating requirement provided by the geothermal system from the total building heat load (with a COP = 1 for the backup system):

$$\dot{W}_b(t) = \dot{Q}_{build}(t) - \dot{Q}_{build,HP}(t) \quad (4)$$

The power required for heat transfer fluid circulation depends on the head loss and flow rate in the piping network of the borefield. It is thus a function of the piping layout, which depends on the distance B between boreholes, their depth and the number of boreholes. The borefield grids considered in the present work have a number N_x of boreholes in x direction, and N_y in the y direction, as shown in Fig. 1. All boreholes are connected in parallel and are assumed to experience the same fluid mass flow rate (balancing valves employed to achieve equally distributed flow). Although Fig. 1 shows a direct return configuration, it should be noted due to the simplifying assumptions of the head loss calculations, a reverse configuration would yield the same pumping power. Each row of boreholes aligned in the x-direction is connected and then, the final y-column of boreholes collects all x-rows (see Fig. 1). In order to simplify the problem and limit the number of design variables, no piping diameter optimization was attempted. The head loss by unit length was assumed to be equal to $\Delta P' = 0.4$ kPa/m for all pipes, a typical value often used in network design methodology [12]. Then, a constant fluid mass flow rate $\dot{m}_f$ of 0.2 kg/s in each borehole was considered, and the mass flow rate in all branches of the pipe layout was determined. Finally, the power required for fluid circulation is estimated by:

$$\dot{W}_p = 2\left[N_x N_y \left(\frac{\Delta P' H \dot{m}_f}{\rho_f} \right) + N_y \sum_{i=1}^{N_x} \left(\frac{\Delta P' B \left(i \dot{m}_f \right)}{\rho_f} \right) + \sum_{i=1}^{N_y} \left(\frac{\Delta P' B \left(i N_x \dot{m}_f \right)}{\rho_f} \right) \right] \quad (5)$$

The first, second, and third terms on the right-hand side of Eq. (5) represents respectively the pumping needs to drive the flow in the boreholes themselves, in the connected row branches, and in the column-oriented collector. The factor 2 is to account for the return loop. Note that no minor losses were included in this simple head loss model.

In the end, the total power requirement at a given time is the summation of that for the heat pump, the backup system and the circulation pump:

$$\dot{W}_{tot}(t) = \dot{W}_{HP}(t) + \dot{W}_{b}(t) + \dot{W}_{p} \tag{6}$$

The evaluation of energy cost was based on local rates (Hydro-Quebec business rate "G") in which monthly energy consumed is considered [13]. The power distribution is integrated over a month to obtain monthly energy consumption,

$$W_{tot} = \int \dot{W}_{tot}(t)\, dt \tag{7}$$

The cost of energy that was considered is 8.78 ¢/kWh for the first 15,090 kWh, and 4.85 ¢/kWh for remaining monthly consumption. To obtain an annual cost for energy, the monthly costs must be summed up (12 months):

$$C_a = \sum_{i=1}^{12} C_{energy,i} \tag{8.a}$$

with:

$$C_{energy,i} = \begin{cases} W_{tot,i} X_{pE1} & \left(W_{tot,i} \le 15{,}090\ kWh\right) \\ 15.09\times10^{6} X_{pE,1} + \left(W_{tot,i} - 15.09\times10^{6}\right) X_{pE,2} & \left(W_{tot,i} > 15{,}090\ kWh\right) \end{cases} \tag{8.b}$$

In the equations above, $W_{tot,i}$, is the total energy consumed for month *i* in kWh, X_{pE1}, the energy cost [$/Wh] for the first 15,090 kWh consumed and X_{pE2}, the energy cost for remaining kWh if monthly total is over 15,090 kWh. Even though the building load remains essentially unchanged from year to year, the annual operating cost of the geothermal heat pump system varies over the years as ground temperature is evolving in time. In general, heat pump performance tends to decrease in time, and thus, more energy needs to be supplied to the heat pump.

2.2 Initial cost

The initial cost is the summation of the costs of the heat pump, drilling, excavation and piping:

$$C_{initial} = C_{HP} + C_{drill} + C_{ex} + C_{pipe} \quad (9)$$

The heat pump purchase cost is a function of its design load capacity, i.e. the maximal heating load that could be delivered to the building by the heat pump. In the present paper, the heat pump cost is evaluated by a recently developed correlation [14].

$$C_{HP} = 1949.5 \times q_{heating}^{0.665} \quad (10)$$

where $q_{heating}$ is the maximum heat load carried out by the heat pump [kW].

Note that in the present cases tested, no initial cost for the backup system is taken into account. This could correspond to different situations such as an existing building with its heating/cooling system already in-place where or a building for which the size reduction of the heating/cooling system is not significant when installing a geothermal system (e.g., when only a small portion of the load is taken by the geothermal system). Depending on the context, the backup system cost can be added if it is of importance to the problem. It would likely depend strongly on the type of backup system considered.

Drilling cost depends on the number of boreholes and on their depth. Assuming a drilling cost per meter X_d [$/m], and boreholes with a depth H, one finds:

$$C_{drill} = N_x N_y H X_d \quad (11)$$

Excavation is required in order to install collecting pipes. The excavation cost was evaluated by considering that a trench was needed for every row in the x-direction (Fig. 1) to link boreholes together, with an additional trench to join rows to the mechanical room in the y-direction. A survey among local excavation contractors allowed to evaluate excavation cost between 40 and 65 $ per m^3 of ground removed. In the present work, we used trench dimensions of 0.6 m of breadth and 1.2 m of depth. Therefore, the lineic cost of excavation could be evaluated between 32 $/m and 47 $/m. In the present work, an average value of 42 $/m was retained. Therefore, the excavation cost could be evaluated by:

$$C_{ex} = \left[N_y \left(N_x B \right) + \left(N_y B \right) \right] X_{ex} \quad (12)$$

where X_{ex} is the excavation price per length of trench, i.e. in the present case 42 $/m.

Piping cost depends on the length needed, which is related to the number of boreholes and distance between them. Based on Fig. 1, total piping length can be estimated by

$$L_{pipe} = 2\left[N_x N_y B + N_y B + N_x N_y H \right] \quad (13.a)$$

Since the diameter of each pipe in the layout might be different, their actual cost per unit length would likely be different. However, since pipe diameter are often of the same order of magnitude in geothermal applications, and in order to simplify the model, a constant but representative cost X_{pipe} per unit length of piping was used. Therefore, the cost for the piping is:

$$C_{pipe} = L_{pipe} X_{pipe} \quad (13.b)$$

The cost for piping will have the effect of limiting the footprint of the optimized borefield: distant boreholes will provide a better heat transfer performance, but will also require more piping. Note that if the footprint area required by the borefield is an important constraint in a project, an additional "cost on land" could also be included in the initial cost. All numerical values required in the above-mentioned equations are provided in Tables I and II.

3. Mathematical model of borehole ground heat exchanger

To evaluate the objective function (total cost) for a given design, borefield simulations must be performed to determine the geothermal heat pump transient performance and operating cost. Our borehole heat transfer model was developed in Matlab and is based on current up-to-date practices. Because long-term effects are considered, a finite line-source (FLS) approach is adequate [15] [16] [17], and can properly capture axial effects. Since vertical ground heat exchanger simulations with this model are already documented in literature, only a brief explanation is proposed here. An average temperature value at a borehole wall can be determined by integrating the temperature distribution achieved from the FLS model over its axial extent (z axis). In this paper, we used the formulation developed in [18], which is not repeated here for the sake of conciseness. In practice, each borehole is subject to a heating/cooling load which varies in time, and that can be represented as a series of heat pulses occurring at each time step. To determine the temperature at a given time and position, the superposition principle can be invoked thanks to the linearity of the conduction equation [19][20][16]. In order to speed up the resolution, Ref. [20] developed a procedure based on Fast Fourier Transform, or "FFT",

(which we used in the present work) in which the equation to determine the temperature increase at a borehole wall is seen as a convolution product [21] of incremental loads and FLS solutions. In the case of a borefield, the effect of each borehole on the other boreholes can be summed in order to determine the actual temperature at the surface of each borehole, provided that the transient heat load for each borehole is known (superposition principle). Finally, the heat transfer fluid temperature evolution can be related to the temperature at the surface of the borehole and to the heat load via a borehole thermal resistance.

What is usually known when designing a geothermal system is the total heating and cooling load of the building, not directly the heat transfer rates at each borehole or to the borefield. Building and borefield loads are related via the COP of the heat pump, but the effective COP is a function of the heat transfer fluid temperature. Assuming that the total building heat load is known, the incremental load at each borehole is not available a priori since the effective COP and the borehole-to-borehole interactions are not known. In the present paper, an iterative procedure was developed to determine the actual heat supplied by each borehole of the grid. The proposed method is illustrated in Fig. 2.

The initialization consists in defining borehole parameters, as well as the grid geometry. All unit thermal responses (with subsampling method [20]) and their Fourier transforms can be calculated. An initial guess for the entering water temperature to the heat pump at all times must be specified. Then, the following steps are followed:

Step 1: The heat pump COP at all time steps is calculated as a function of the entering water temperature according to the correlation developed in [4]. Note that although this correlation is widely used, it does not account for the fact all heat pumps are designed for a specific range of entering water temperatures. Said differently, in practice too high or too low entering water temperatures cannot be dealt with by the heat pump system. The correlation, on the other hand, returns COP values even when the temperature is low or high, and could thus be somewhat imprecise or misleading when non-typical values of temperature are used. Future work could consider constraints on heat pump specifications or performance curves for specific heat pump models.

Step 2: The total heat supplied by the borefield at each time step is determined from the COP and building heat load values,

$$Q_{borefield} = \left(1 \pm 1/COP\right) Q_{design} \tag{14}$$

where the sign is positive for cooling and negative for heating.

Step 3: The fluid inlet temperature to the boreholes (i.e., the fluid outlet temperature at the heat pump) is calculated. It is assumed that all boreholes are connected in parallel in such a way that they all receive the fluid at that temperature and there is not heat loss or gain between the heat pump and the boreholes. Based on energy conservation, it follows that:

$$T_{f,in} = \frac{Q_{borefield}}{n\dot{m}_f c_f} + \overline{T}_{f,out} \tag{15}$$

where n is the number of boreholes in the grid. Then, a uniform load distribution among the boreholes is first assumed in order to estimate an outlet fluid temperature at each borehole. In this case, the outlet fluid temperature of all boreholes ($\overline{T}_{f,out}$) is simply the entering water temperature to heat pump. So,

Step 4: The heat transfer rate provided by each borehole i is calculated from energy conservation:

$$Q_{b,i} = \dot{m}_f c_f \left(T_{f,in} - T_{f,out,i}\right) \quad \text{for} \quad i = 1, n \tag{16}$$

Then, it is assumed that each borehole experiences the same fraction of the total heat load calculated in Step 2. Actually, an initial model was developed to account for the non-uniformity of the load distribution among boreholes, but it was found that it had virtually no effect on the results, so it was decided to simplify the model with a uniform distribution in this paper. To reduce the computational time, only « unique » boreholes are considered, i.e. the calculations are not repeated for boreholes with the same set of distances to other boreholes. In other words, the index “i” refers to each borehole that has a unique position in the grid. No attempt was made to use symmetry groups.

Step 5: Incremental load $q_{b,i} = \left(Q_{b,i_t} - Q_{b,i_{t-1}}\right) / H$ for each borehole i, and its Fourier transform, is calculated. Matlab pre-programmed algorithm “FFT” was used to evaluate discrete Fourier transforms [20].

Step 6: In order to obtain the borehole wall temperature $T_{b,i}$ for each borehole i, time superposition is performed by multiplying two Fourier times series: borehole thermal

response function with incremental load applied (convolution theorem, FFT-S method [20]). Note that spatial superposition is performed once on thermal response function before entering the iterative process with borefield load being assumed distributed uniformly (see, step 4). Thus the thermal response of the borefield is not considered as a whole that is calculated by the FFT. The iterative procedure was implemented with the FFT approach on each individual borehole, without fixing bore surface temperature. As the finite line source model is used, the surface temperature is uniform for each borehole, but each borehole has a different temperature in our model.

Step 7: Then, the average fluid temperature in each borehole is calculated:

$$\bar{T}_{f,i} = \frac{Q_{b,i}}{H} R_b^{'} + T_{b,i} \tag{17}$$

where $R_b^{'}$ is the borehole thermal resistance per unit of length [mK/W]. The borehole resistance was calculated from shape factors ([22],[23]). A value of 0.1076 mK/W was obtained for heating mode, and 0.1082 mK/W for cooling.

Step 8: From the fluid mean temperature in each borehole, an exit temperature can be calculated for each borehole:

$$T_{f,out,i} = \bar{T}_{f,i} - Q_{b,i} \Big/ \left(2\dot{m}_f c_f \right) \tag{18}$$

Therefore, even though the heat load is the same for each borehole, the exit temperature calculated is different because it is based on the borehole wall temperature which depends on each different thermal response.

Step 9: Once exit fluid temperature for each borehole $T_{f,out,i}$ is calculated, a new updated entering water temperature to the heat pump is calculated:

$$\bar{T}_{f,out}^{new} = \frac{1}{n} \sum_{i=1}^{n} T_{f,out,i} \tag{19}$$

Then, one returns to step 1, where the COP is calculated according to the borefield outlet average temperature (after mixing of streams coming out of all boreholes). The procedure is repeated until convergence is achieved, i.e. once $\bar{T}_{f,out}$ stops to change between consecutive iterations. The following criterion was used to declare convergence:

$$\left| 1 - \frac{\dot{m}_f c_f \left(T_{f,in} - \bar{T}_{f,out} \right)}{Q_{borefield}} \right| \leq 0.001 \tag{20}$$

In the end, the transient evolution of the heat pump COP, along with the inlet and outlet fluid temperatures and heat transfer rate at each borehole are determined. The overall performance of the system can be evaluated by calculating the energy consumed by the heat pump.

4. Borefield optimization procedure

The total cost, Eq. (2), is the objective function to minimize. The design variables that were considered for this purpose are the following:

- Depth of boreholes (H): All boreholes were assumed to have the same depth. The bounds for this design variable were chosen in accordance with the current practice[4]. The lower bound was set to 45 m, and upper bound, to 105 m;
- Distance between boreholes (B): The distance B corresponds to the center-to-center distance between two consecutive boreholes, and it is assumed to be the same in the x and y directions, see Fig. 1. This values for this design variable was limited between 3 m and 8 m [6];
- Percentage of the building peak load assumed by the geothermal heat pump system (p): As mentioned previously, this percentage was used to cut off or "shave" the transient building load in periods of high heating demand, using a backup system to supply the exceeding energy requirement. Values of p were limited between 60% and 90%;
- Number of boreholes in the grid and boreholes arrangement (e.g., 2×3 versus 3×2): Only aligned grids of boreholes were considered, i.e. no staggered boreholes.

The optimization was performed by using the Matlab optimization routine "fmincon" [24]. This minimization algorithm could be used straightforwardly to optimize the design variables H, B and p, all of which are continuous variables. However, the number of boreholes in each direction can only take discrete values. In order to simplify the optimization strategy, a predetermined N_x by N_y grid of boreholes was assumed, and then, the three continuous variables p, B and H were optimized for that particular layout. Next, N_x and N_y were changed, and the continuous variables were optimized again. In the end, the minimal cost of a series of grid patterns was determined and a comparison

between the results allowed to determine the best grid (i.e. the value of N_x and N_y that minimize the total cost).

In order to limit the number of possible borehole grids to simulate and to provide realistic results, certain constraints were invoked. First, the number of boreholes in one direction must be equal or lower than three times the number of boreholes in the other direction ($N_x \leq 3N_y$ or $N_y \leq 3N_x$). This constraint was invoked to consider scenarios where the shape of the borefield footprint is an issue, and the value "3" was chosen arbitrary to illustrate the methodology. Nevertheless, one could adapt the constraint to the specific needs of a given project. In fact, when the land where the borefield is to be installed is vast enough, this constraint can even be disregarded.

Also, for a given project, a maximal and a minimal number of boreholes were calculated based on an acceptable range of maximal load per unit of total length (between 30 and 130 W/m) for the entire borefield, i.e.:

$$30 \leq \frac{\dot{W}_{field\_heating\_peak}}{NH} \leq 130 \tag{21}$$

All combination of N_x and N_y respecting these constraints were simulated.

With the proposed procedure, an optimization for a given $N_x \times N_y$ configuration run on a CPU Intel P4 (1 Go RAM, 3.2 GHz) is achieved in 5 to 15 minutes.

5. Example of minimized total cost of optimal designs

A synthetic building load was generated based on [20][17]. The resulting transient building load is shown in Fig. 3, and this load was used as an input to the optimization procedure described above. In order to show the most influential parameters of Eq. (1), a ventilation of the total cost is presented in Fig. 4a for an optimized system with a 3×2 grid, and with a ground thermal conductivity of 3 W/mK. Note that for this borefield configuration, the minimized cost $C_{tot,min}$ was 113,270$. The total cost of hypothetical conventional system (electric) was calculated, and was found to be around 168,500$. That cost was achieved by calculating the cost of energy for heating (no back-up cooling system was considered, and no cost for the heating equipment was counted). There is thus a reduction of 49% of the total cost with the geothermal system under the present assumptions.

It can be seen in Fig. 4a that the operating cost (i.e., energy) is dominant compared to the initial cost (62% vs. 38% respectively), and that excavation and piping costs are marginal in the present optimized design. This means that the algorithm produced a relatively compact borefield, and thus low excavation/piping costs. Heat pump and drilling have similar weights in the optimal allocation of costs, the heat pump being slightly more expensive.

The same exercise was performed for thermal conductivities ranging from 1.5 to 4.5 W/mK and for borefield configurations of 2×2, 2×3, 4×2 and 3×3. For all situations, even if the value of the total cost was different, its ventilation was similar to that of Fig. 4a with variations of only ±4%.

6. Effect of ground thermal conductivity

The effect of ground thermal conductivity on optimal design variables and minimal costs was investigated. In order to do so, the total cost of a given project was minimized based on the procedure described in the sections above, for a series of different ground conductivity values (1.5, 2, 2.5, 3, 3.5, 4, and 4.5 W/mK). The transient load of Fig. 3 was used. For that load, the minimal number of boreholes was estimated at 4, and maximal number at 9, which allows the following configurations to be considered: 2×2, 3×2, 4×2 and 3×3 according to the geometrical constraint explained above.

The minimized cost is presented in Fig. 5 as a function of ground conductivity and borehole arrangement, and detailed cost ventilation is reported in Table III. As could be expected, the overall cost is reduced when the thermal conductivity of the environment where the vertical heat exchanger is installed increases. For example, considering the 2×2 arrangement, there is a total cost reduction of 17,340$ when the conductivity changes from 1.5 to W/mK to 4.5 W/mK (~14% cheaper). This saving is first due to the reduction of the operating cost when ground conductivity increases. In a more conductive environment, the ground thermal resistance is reduced, and as a result, the overall heat pumps system works more efficiently. The saving in highly conductive environment is also caused by the reduction of drilling costs, since the required borehole length becomes smaller due to a larger heat transfer rate per unit length of borehole. In the present model, the drilling cost can represent up to 40% of the initial investment (Table III) and it tends

to decrease when conductivity increases in optimized designs. Having shorter boreholes also contributes to reducing piping costs. On the other hand, when the conductivity is higher, the heat pump tends to become larger (and thus more expensive) in optimized designs since the percentage of the total load assumed by the borefield increases. However, this augmentation of cost is balanced by other cost reductions. For example, in Table III, heat pump cost increases by about 3600$ between 1.5 and 4.5 W/mK and drilling cost decreases of 4200$ for the 3×2 configuration.

Comparing configurations with 6 (3×2) and 8 (4×2) boreholes, one notices that a smaller number of boreholes was found to be better in the present case. Both grids have a very similar performance, their annual costs being close for conductivity higher than 2.5 W/mK, and both grids having similar heat transfer rate per unit length at a given conductivity. Boreholes in the 8-borehole grid tend to be closer (shorter distance B) which results in smaller pipe cost and in smaller excavation cost per borehole than with the 6-borehole grid. However, when the number of boreholes is higher, the total cost remains high even if the price per borehole is smaller. Therefore, for the present test case with configurations 2×2 to 3×3, a smaller number of deeper boreholes was more valuable than many shallower boreholes. Note that a 2×1 grid was also tested, and proved to be more expensive than the other configurations, in particular for thermal conductivities below 3 W/mK (out of range in Fig. 5). This suggests that only two boreholes is too small a number from an economic point of view in the present case.

Cost minimal designs were also compared with ASHRAE's recommended formula for determining borefield required length [6]. In that method, the heat load that will be assumed by the borefield must be specified by the designer, whereas with the present methodology, it is determined based on cost minimization (i.e., varying p to minimize the overall cost). To calculate the required length based on ASHRAE's method, it was decided to use the "optimized" heat load to the borefield that had been achieved by the economical optimization procedure. This offers an interesting basis of comparison, but it should be remembered that in the ASHRAE's method, the heat load to the ground is not optimized but imposed by the designer. The parameters involved in ASHRAE's sizing procedure such as inlet-to-outlet temperature difference, average annual power to the ground, part load factor, heating design load, and power consumed at heat pump were

thus taken from the economical optimization results. The short-circuit factor and penalty temperature were taken from Tables in [6], and respective values of 1.05, and 0.8°C were found to be adequate. Figure 6 shows a comparison between the total length obtained from the optimization process and the length recommended by [6] for configuration 3×2. It can be seen that the optimized length based on cost has a tendency to be slightly smaller for low conductivities, and slightly larger for higher conductivities.

7. Economics of thermal response tests

The optimization process detailed in Section 4 was used in order to evaluate the economical benefits of performing a thermal response test (TRT) when sizing a borefield [25][26]. TRTs are performed to measure the average ground thermal conductivity value, which is then used to determine the required boreholes length and number. In a test borehole, heat is injected at a constant rate for 2 to 3 days while fluid temperature is recorded. Then, the temperature evolution is fitted with an analytical solution in order to establish the equivalent ground conductivity around the borehole. TRTs can be expensive to perform since they involve drilling a test borehole, transporting TRT equipment on site (heater, pump, etc.), and recording for up to 72 hours of data. That is why they are not always used in practice. TRTs are typically performed for projects involving a large number of boreholes.

In this section, we propose a methodology to estimate the economical benefits of a TRT (see Fig. 7). The procedure consists in, first, optimizing the geothermal system based on "real" ground conductivity value, k_{real}, with the algorithm presented previously in order to achieve a cost minimal design. Using the actual ground conductivity in the optimization run implies that this value has been determined precisely from a TRT. Then, two more design optimization runs are performed: one with a conductivity value higher than the actual one ($k_{real} + \Delta k$), and another with a conductivity smaller than the real one ($k_{real} - \Delta k$). The two obtained designs correspond to the "best" designs that would be possible if the ground conductivity was known to be $k_{real} + \Delta k$ and $k_{real} - \Delta k$. The range of conductivity investigated (i.e., Δk) should correspond to the plausible range of ground conductivity when no TRT is performed, based on the geological materials. Based on the location of the borehole and existing geological data, it is often possible to provide a

certain estimate or a range of possibilities for k, even though a precise value is not available. Finally, these two designs (i.e., number of boreholes, bore length, etc., optimized for $k_{real} \pm \Delta k$) are simulated with the real conductivity and the corresponding total costs are determined. These costs are expected to be higher than the one of the system that was designed for the real conductivity, since the corresponding systems were optimized or designed based on a different conductivity value. The additional cost can be seen as the economical gain that a TRT could provide by narrow down the plausible conductivity range to a more precise value, and could be compared to the actual investment required to perform the TRT. In other words, if the cost of the TRT is higher than the potential saving resulting from pinpointing an exact conductivity value, then, there is no point in performing one for the project of interest. In that case, it would be more profitable to simply design the system without knowing exactly the ground conductivity.

This proposed procedure was applied to the test case presented in Section 6. For the sake of illustration, uncertainties of ±33% were considered. Results are shown in Fig. 8 for a 3×2 grid. As seen in Fig. 8, the maximum project cost difference between TRT optimized design (blue curve) and error designed borefield (red and green curves) occurred at 1.5 W/mK and is around 3000$ for an error of −33%. This cost difference represents a saving possibility when performing a TRT, but its value is relatively small compared to the cost of a TRT. Without a TRT, ground conductivity can be under or overestimated. If conductivity is underestimated, the geothermal system will be overdesigned, and the initial cost will be greater than it should be. However, the system will be performing better than expected (due to overdesign) and the energy cost will go down, thus balancing to some extent the high initial investment. If conductivity is overestimated, the system will be under designed, resulting in a higher energy cost that is balanced to some extent by the smaller initial investment. In the present case, if the error on thermal conductivity estimation is ±33% or less, the decision of performing a TRT does not seem to be sound from an economical standpoint. One should note that the cost difference between curves of Fig. 8 becomes smaller for higher conductivities. This demonstrates that the impact of conductivity is less significant in conductive grounds.

This effect is also observed in Fig. 5 where the slope of the minimized cost versus ground conductivity decreases with k.

Despite the previous comment on the necessity (or non-necessity) of TRTs, it is important to recall that it holds only for the present test case, which is a relatively small borefield, and under the various assumptions that have been made. As more boreholes are added, there is a point where it becomes economically beneficial to determine precisely conductivity. A methodology was thus developed in order to establish the threshold from which a TRT seems beneficial economically. The method is based on the procedure illustrated in Fig. 7 and described previously. The number of boreholes was increased and for each situation, the additional total cost associated with the uncertainty on k was determined as explained before. The total borefield load was adapted to the number of boreholes by maintaining a constant load per borehole. The excess cost due to uncertainty is presented in Fig. 9 as a function of the number of boreholes. It can be seen that the excess cost increases with the number of boreholes. Depending on the local cost of TRTs and on the specificities of a project (e.g., cost of energy, estimated conductivity and error, load, etc.) a similar figure can be built in order to establish whether a TRT should be performed or not.

Even though the minimized cost is very similar for different estimated values of conductivity, the designs obtained can be quite different. For example, Fig. 10 presents the three design parameters (H, B, p) minimizing the total cost for the three conductivities: –33% of error, +33%, compared to actual TRT value of k = 3 W/mK. The vertical axis is reported in percentage of the value obtained for the actual TRT case when conductivity is known precisely. It can be seen that when estimating higher value of thermal conductivity, H and B will be smaller (under-design) as ground is expected to be more conductive than it really is. Inversely, when conductivity is estimated smaller than its real value, optimal depth and separation distance will be larger in order to deal with deteriorated heat conduction. Therefore, different optimal designs for different conductivities can yield similar total costs.

8. Impact of transient load profile

The optimization procedure presented in Section 4 was also tested for different building loads. In this section, a comparison between two types of loads on the optimization results is presented: the first type corresponds to the one used in the previous section (Fig. 3), and the second is a constant heating load during the heating season (September to April) with no cooling load. The latter type of load is often preferred in Canadian geothermal systems for commercial or institutional applications. In that case, the geothermal heat pump only assumes a small portion of the total building load and works during the heating season at nearly constant conditions. The steady heating load value was fixed to 30 kW which is around the average heating load of Fig. 3. Optimization results for both loads with a ground conductivity of 3 W/mK are presented in Table IV and the minimized total cost for both loads applied to different grids is shown in Fig. 11.

From Table IV, one can see that total and operational costs tend to be higher for the second type of load profile (constant heat load during heating season) than for the first. This is likely caused by the absence of cooling during summer, i.e. no thermal restitution in the ground. Therefore, ground tends to get cooler and cooler every year, and the overall performance deteriorates. This is also revealed by the optimal values of B achieved for that case which are higher (actually reaching the upper bound for that variable) than for the first profile.

On the other hand, the initial cost is higher for the first type of profile than for the second. This is mainly related to the purchase of the heat pump. In the optimization runs with the constant heating load profile, the allowed upper bound is reached for the design variable p (percentage of the peak) (i.e. 90%, see Table IV). Since the second load evolution is completely flat, that percentage corresponds only to 27 kW since the maximal (and constant) heating load is 30 kW. For the first profile, the optimal percentage obtained by cost minimization is around 75%, but since the peak is around 40 kW, that corresponds to approximately 30 kW. Therefore, in the present analysis, the heat pump capacity needs to be higher for the first type of profiles, and is thus more expensive. Note that the maximal percentage of the peak load assumed by the geothermal system was limited to 90% in the present study, since current practices for commercial and institutional applications tends to limit this value to avoid the heat pump to operate in

under-design conditions and limit the initial costs. On the other hand, this value could be adjusted to each project to limit or not the range of possibilities if required.

Finally, it is interesting to note that, for most of the grids tested, the optimal bore depth was actually similar with both profiles. Furthermore, when the number of boreholes becomes too large, the lower bound for H was obtained (i.e. 45 m for the 3×3 grid). Although this is an indication that such a grid is not optimal and has too many boreholes, the minimized total cost is only slightly higher than for the best grid. This reveals "design robustness" in the sense that several different designs can provide a similar level of performance and that small changes to a design do not result in a drastic drop of performance.

Note that for the first type of heat load profile, the peak load per unit length achieved by the optimal design is around 70 W/m, while for the second profile, it is around 66 W/m. These values are slightly higher than what is typically recommended (e.g., 38 to 58 W/m). Recommendations in literature are generally based on performance or energy aspects, whereas the proposed procedure in this paper is economical. For the test case considered, the economical optimization thus tends to under-size the geothermal borefield compared to present rules of thumb. In the present case, it generated savings on initial cost, without compromising too much the borefield yearly performance. However, this result should be taken cautiously, and cannot be applied straightforwardly to other projects. The procedure outlined in this paper should be applied appropriately with the specificities of these geothermal projects (ground properties, local cost of energy, etc.). It is worth to point out that the "concept" envisioned by the designer (i.e., *how* the geothermal will be used) will impact on cost. As an example, this section tested two types of load profiles applied to the borefield, and as described above, the optimal designs and costs were different. In other words, the designer can also optimize his/her concept in order to minimize overall cost in a given context.

9. Cost sensitivity to design parameters

Based on the above-mentioned results, it is not obvious to determine which design variable has the most influence on the total cost. For that reason, the half-normal plot method [27] was used to investigate the sensitivity of the total cost to the variations of the

design variables: the effects on the total cost of each parameter combination for given conditions is plotted with a normal probability scale on y-axis to identify parameters that have to most influence on the total cost. The results are shown in Fig. 12a for borefield configuration with number of boreholes N ranging from 4 (2×2) to 9 (3×3), submitted to the load of Fig. 3, and simulated in a ground with a thermal conductivity of 3.5 W/mK.

With this qualitative method, the points far from the y-axis, or out of the distribution, are the parameters or combinations of parameters that have the most effect on the cost function. Those points were identified in Fig. 12a as being parameters H and N, and the product HN. This confirms that the number of boreholes influences significantly the total cost as pointed out in Section 6 (Fig. 5). Also, this means that the borehole depth is the other most influential variable. The variation of combined parameters H and N when designing a borefield is also an influencing parameter on the total cost.

The analysis of Fig. 12a reveals that the separation distance B has a less marked impact on total cost compared to effects of H and N. This is probably because B only varies from 3 to 8 m and that the number of boreholes is restrained. The results are different when the number of boreholes is considerably higher. Fig. 12b shows half-normal plot for 20 (5×4) to 28 (7×4) boreholes in borefield submitted to transient load of Fig. 3 multiplied by a factor 3.5, in the same ground. Again, the product HN has a major influence on total cost. For that situation, B is also an influential parameter, as piping and excavation costs become more important. Actually, it can be seen in Fig. 12b that the effect of variables and their products is more evenly distributed than in Fig. 12a. Beside B and product HN, other parameters or products have an effect of the same order of magnitude on total costs. This suggests that the more boreholes there are in a grid, the more all design parameters will have significant effects on the total cost.

10. Conclusions

The main objective of this paper was to develop a new design method in order to size and design vertical ground heat exchangers coupled to a heat pump. The procedure relies on total cost minimization, and includes a series of different initial costs (e.g., drilling, excavation, heat pump, and piping network) as well as the operation cost (energy).

Although the heating and cooling needs of the building have to be specified, the method optimizes the repartition of this demand between the geothermal heat pump and a back-up system. In the end, the procedure allows to achieve the best design in a given economic context.

Additionally, the design strategy has been used to evidence how ground thermal conductivity influences the total cost of a project and its optimal ventilation among the different budget items. We also proposed a method to determine the economical benefit (or loss) of performing a thermal response test to pinpoint the ground conductivity value in a given context. Below a certain number of boreholes, the benefits of knowing k precisely are too small compared to the cost of a TRT. The sensitivity of the total cost to variations of the design variables was investigated, and the number of boreholes and their depth were the most influencing parameters for the case considered.

The method could be used in a variety of contexts and applications, and could easily be adapted to include other costs and constraints that were not considered here. Future work could focus on determining general trends of optimal designs in different cases in order to help designers to achieve better performance over the lifetime of their geothermal projects, and thus, help to a greater deployment of this technology.

Acknowledgements

This work was supported by the Fonds de Recherche Québécois-Nature et Technologies (FRQNT).

References

[1] A. Mustafa Omer, "Ground-source heat pumps systems and applications," *Renewable and Sustainable Energy Reviews*, vol. 12, no. 2, pp. 344–371, Feb. 2008.

[2] I. B. Fridleifsson, "Geothermal energy for the benefit of the people," *Renewable and Sustainable Energy Reviews*, vol. 5, no. 3, pp. 299–312, Sep. 2001.

[3] J. W. Lund, D. H. Freeston, and T. L. Boyd, "Direct utilization of geothermal energy 2010 worldwide review," *Geothermics*, vol. 40, no. 3, pp. 159–180, Sep. 2011.

[4] RETScreen International, "Clean Energy Project Analysis : RETScreen Engineering and Cases Textbook, Ground-source Heat Pump Project Analysis Chapter." Minister of Natural Resources Canada, 2005.

[5] S. J. Self, B. V. Reddy, and M. A. Rosen, “Geothermal heat pump systems: Status review and comparison with other heating options,” *Applied Energy*, vol. 101, pp. 341–348, Jan. 2013.
[6] American Society of Heating, Refrigerating, and Air-Conditioning Engineers, Inc., “Handbook of Applications, Chapter 32.” ASHRAE, 2007.
[7] S. Kavanaugh and K. Rafferty, *Ground-Source Heat Pumps - Design of Geothermal Systems for Commercial and Institutional Buildings*. Ashrae, 1997.
[8] S. Belanger and L. Gosselin, “Multi-objective genetic algorithm optimization of thermoelectric heat exchanger for waste heat recovery,” *International Journal of Energy Research*, vol. 36, no. 5, pp. 632–642, 2012.
[9] B. Allen, M. Savard-Goguen, and L. Gosselin, “Optimizing heat exchanger networks with genetic algorithms for designing each heat exchanger including condensers,” *Applied Thermal Engineering*, vol. 29, no. 16, pp. 3437–3444, 2009.
[10] B. Allen and L. Gosselin, “Optimal geometry and flow arrangement for minimizing the cost of shell-and-tube condensers,” *International Journal of Energy Research*, vol. 32, no. 10, pp. 958–969, 2008.
[11] P. Wildi-Tremblay and L. Gosselin, “Minimizing shell-and-tube heat exchanger cost with genetic algorithms and considering maintenance,” *International Journal of Energy Research*, vol. 31, no. 9, pp. 867–885, 2007.
[12] F. C. McQuiston, J. D. Parker, and J. D. Spitler, *Heating, ventilating, and air conditioning: analysis and design*. John Wiley & Sons, 2005.
[13] Hydro-Quebec, “http://www.hydroquebec.com/fr/index.html.” .
[14] R. Croteau and L. Gosselin, “Correlation for cost of ground coupled heat pumps as a function of heating/cooling capacities and COP,” *International Journal of Energy Research*, Submitted 2013.
[15] M. Philippe, M. Bernier, and D. Marchio, “Validity ranges of three analytical solutions to heat transfer in the vicinity of single boreholes,” *Geothermics*, vol. 38, no. 4, pp. 407–413, Dec. 2009.
[16] P. Eskilson, “Thermal Analysis of Heat Extraction Boreholes, Ph.D. Thesis.” Mathematical Physics Department, University of Lund, Lund, Sweden, 1987.
[17] D. Marcotte, P. Pasquier, F. Sheriff, and M. Bernier, “The importance of axial effects for borehole design of geothermal heat-pump systems,” *Renewable Energy*, vol. 35, no. 4, pp. 763–770, Apr. 2010.
[18] L. Lamarche and B. Beauchamp, “A new contribution to the finite line-source model for geothermal boreholes,” *Energy and Buildings*, vol. 39, no. 2, pp. 188–198, Feb. 2007.
[19] C. Yavuzturk, “Modeling of Vertical Ground Loop Heat Exchangers for Ground Source Heat Pump Systems, Ph.D. Thesis.” Oklahoma State University, 1999.
[20] D. Marcotte and P. Pasquier, “Fast fluid and ground temperature computation for geothermal ground-loop heat exchanger systems,” *Geothermics*, vol. 37, no. 6, pp. 651–665, Dec. 2008.
[21] E. Kreyszig, *Advanced engineering mathematics*, 9th ed. Hoboken, N.J.: John Wiley & Sons, 2006.
[22] C. P. Remund, “Borehole thermal resistance: laboratory and field studies,” *ASHRAE Transactions*, vol. 105, no. 1, pp. 439–445, 1999.

[23] L. Lamarche, S. Kajl, and B. Beauchamp, “A review of methods to evaluate borehole thermal resistances in geothermal heat-pump systems,” *Geothermics,* vol. 39, no. 2, pp. 187–200, Jun. 2010.
[24] “Matlab Documentation User Guide.” MathWorks, 2012.
[25] J. Raymond, R. Therrien, L. Gosselin, and R. Lefebvre, “A Review of Thermal Response Test Analysis Using Pumping Test Concepts,” *Ground Water*, vol. 49, no. 6, pp. 932–945, 2011.
[26] J. Raymond, R. Therrien, and L. Gosselin, “Borehole temperature evolution during thermal response tests,” *Geothermics,* vol. 40, no. 1, pp. 69–78, Mar. 2011.
[27] C. Daniel, “Use of Half-Normal Plots in Interpreting Factorial Two-Level Experiments,” *Technometrics,* vol. 1, no. 4, pp. 311–341, Nov. 1959.
[28] C. K. Lee and H. N. Lam, “Computer simulation of borehole ground heat exchangers for geothermal heat pump systems,” *Renewable Energy,* vol. 33, no. 6, pp. 1286–1296, Jun. 2008.

Figure captions

Figure 1 Schematic representation of the borefield considered in this study with the connections between boreholes.

Figure 2 Iterative process to simulate heat transfer in the borefield.

Figure 3 Transient heating/cooling load used to perform borefield simulation (negative value for heating load, and positive, for cooling mode).

Figure 4 Total cost ventilation for optimized design for 3×2 configuration.

Figure 5 Minimized total cost as a function of ground thermal conductivity for different grids of boreholes.

Figure 6 Optimized total length of the boreholes as a function of ground conductivity compared to recommended length.

Figure 7 Methodology to evaluate the augmentation of the total cost of a project, ΔC_{tot}, when designing with uncertain ground thermal conductivity.

Figure 8 Minimized total cost of a 3×2 grid for known conductivities (from a TRT) and for uncertain conductivities with variations of –33% and +33%.

Figure 9 Augmentation of cost due uncertainty on ground thermal conductivity versus number of boreholes for square configurations ($N_x = N_y$), with k_{real} = 3.5 W/mK and $\Delta k/k = \pm 33\%$.

Figure 10 Variation of design parameters in percentage of actual values when optimizing with erroneous conductivities with error of –33% and +33%.

Figure 11 Total cost for transient heating/cooling load of Fig. 3 (blue curve) and constant heating load (red curve) for different borefield configurations (see Table IV).

Figure 12 Half-normal plot for total cost function sensitivity to design parameters N, H, B, and p: a) for N = 4 to 9 boreholes; b) for N = 20 to 28 boreholes.

Table I. Values of vertical ground heat exchanger parameters [28].

Parameters	Values	Units
Borehole thermal resistance for heating R_b'	0.1076	m K W^{-1}
Borehole thermal resistance for cooling R_b'	0.1082	m K W^{-1}
Ground thermal diffusivity α_g	1.62×10^{-6}	m^2 s^{-1}
Fluid specific heat c_f	4190	J kg^{-1} K^{-1}
Fluid mass flow rate per borehole $\dot{m}_f$	0.2	kg s^{-1}
Surface temperature	7	°C

Table II. Values of parameters used to calculate total cost (all prices in CAN$).

Parameter	Value	Units
Energy cost of first 15,090 kWh per month X_{pE1}	0.0878	$/kWh
Energy cost remaining kWh per month X_{pE2}	0.0485	$/kWh
Drilling cost X_d [4]	40	$/m
Excavation cost X_{ex}	42	$/m
Piping cost X_{pipe}	3	$/m
Interest rate j	0.06	-
Life-time of the project n	20	years

Table III. Detailed optimization results for different configurations and ground conductivities.

k W/mK	**H_{opt}** m	**B_{opt}** m	**p_{opt}** %	**$C_{tot,min}$** k$	**C_a** k$	**$C_{initial}$** k$	**C_{HP}** k$	**C_{drill}** k$	**C_{ex}** k$	**C_{pipe}** k$
3×2										
1.5	74.2	6.2	60.0	124.3	82.2	42.1	19.7	17.8	1.6	3.0
2.0	75.2	6.6	73.0	119.5	74.4	45.2	22.4	18.1	1.7	3.0
2.5	69.2	6.4	74.7	115.9	72.1	43.8	22.8	16.6	1.6	2.8
3.0	64.7	6.2	75.6	113.3	70.6	42.7	23.0	15.5	1.6	2.6
3.5	61.2	6.0	76.0	111.3	69.5	41.7	23.1	14.7	1.5	2.5
4.0	58.5	5.9	76.9	109.7	68.6	41.1	23.2	14.1	1.5	2.4
4.5	56.4	5.7	77.3	108.5	67.9	40.6	23.3	13.5	1.4	2.3
3×3										
1.5	48.9	5.8	60.0	125.9	83.3	42.6	19.7	17.6	2.2	3.1
2.0	45.0	5.6	61.6	121.2	79.9	41.2	20.1	16.2	2.1	2.8
2.5	45.4	6.0	73.5	117.8	73.7	44.0	22.5	16.4	2.3	2.9
3.0	45.0	5.7	75.4	115.1	71.0	44.1	22.9	16.2	2.2	2.8
3.5	45.0	5.4	76.3	113.2	69.0	44.2	23.1	16.2	2.1	2.8
4.0	45.0	5.2	77.7	111.8	67.4	44.4	23.4	16.2	2.0	2.8
4.5	45.0	5.0	78.6	110.7	66.2	44.5	23.6	16.2	1.9	2.8

Table IV. Optimization results for two different building annual loads.

Transient load (Fig. 3)						
Boreholes	H_{opt} (m)	B_{opt} (m)	p_{opt} (%)	$C_{tot,min}$ (k$)	C_a (k$)	$C_{initial}$ (k$)
4 (2×2)	97.0	6.6	76.4	111.3	69.0	42.3
6 (3×2)	64.7	6.2	75.6	113.3	70.6	42.7
8 (4×2)	48.2	5.9	75.1	114.5	71.6	42.9
9 (3×3)	45.0	5.7	75.4	115.1	71.0	44.1
Constant heating load (no cooling)						
Boreholes	H_{opt} (m)	B_{opt} (m)	p_{opt} (%)	$C_{tot,min}$ (k$)	C_a (k$)	$C_{initial}$ (k$)
4 (2×2)	103.1	8.0	90.0	119.7	81.7	38.1
6 (3×2)	45.0	8.0	90.0	125.6	93.4	32.3
8 (4×2)	49.6	8.0	90.0	123.9	85.0	38.9
9 (3×3)	45.0	8.0	90.0	124.8	85.1	39.7

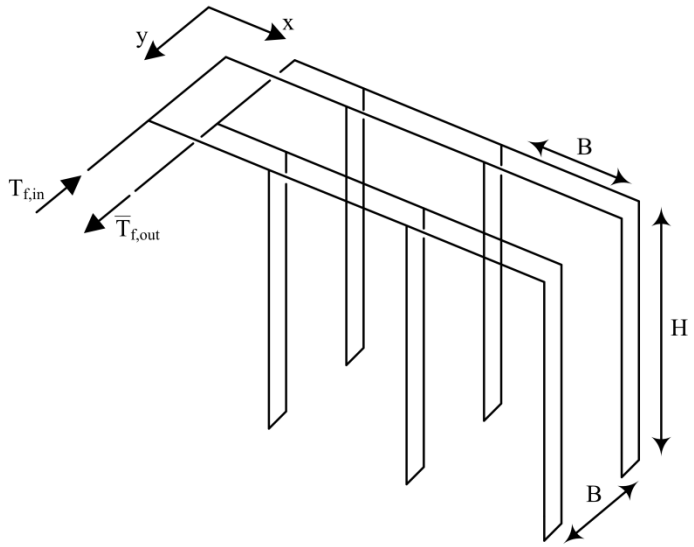

Figure 1

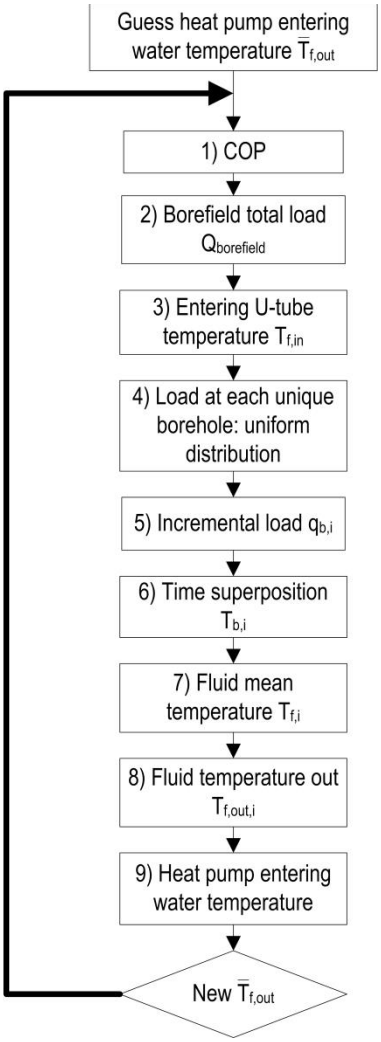
Guess heat pump entering water temperature $\bar{T}_{f,out}$
1) COP
2) Borefield total load $Q_{borefield}$
3) Entering U-tube temperature $T_{f,in}$
4) Load at each unique borehole: uniform distribution
5) Incremental load $q_{b,i}$
6) Time superposition $T_{b,i}$
7) Fluid mean temperature $T_{f,i}$
8) Fluid temperature out $T_{f,out,i}$
9) Heat pump entering water temperature
New $\bar{T}_{f,out}$

Figure 2

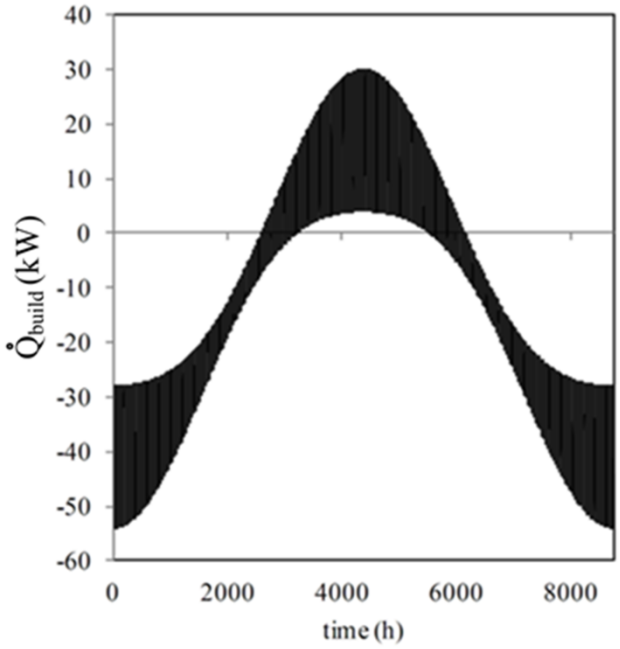
40
30
20
10
0
-10
-20
-30
-40
-50
-60
$\dot{Q}_{build}$ (kW)
0
2000
4000
6000
8000
time (h)

Figure 3

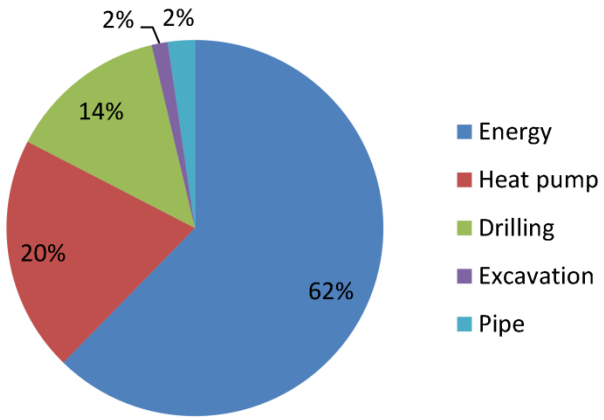

Figure 4

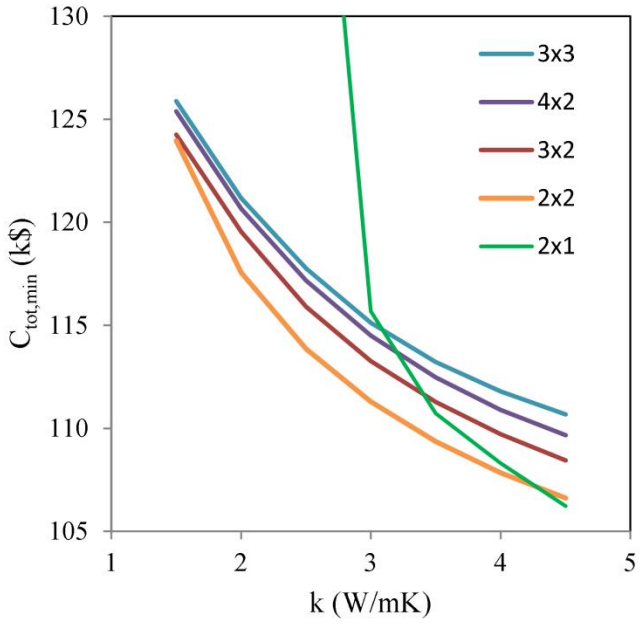
130
125
120
115
110
105
1
2
3
4
5
$C_{tot,min}$ (k$)
k (W/mK)
3x3
4x2
3x2
2x2
2x1

Figure 5

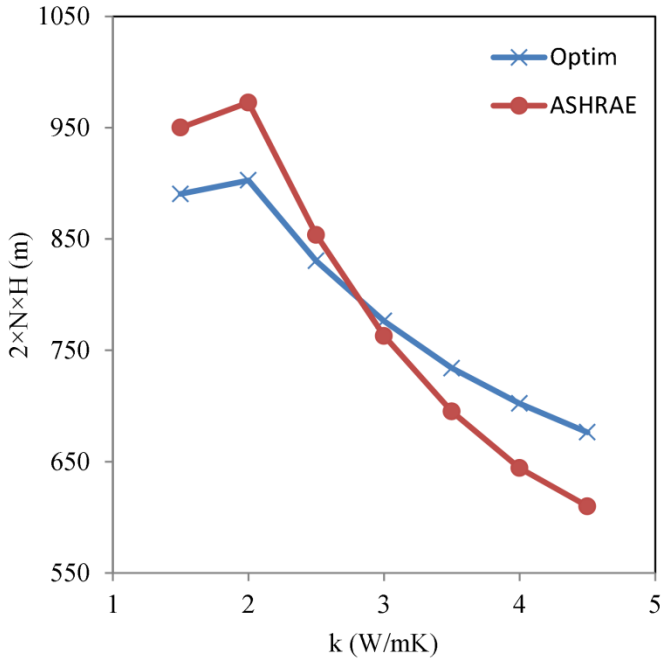

Figure 6

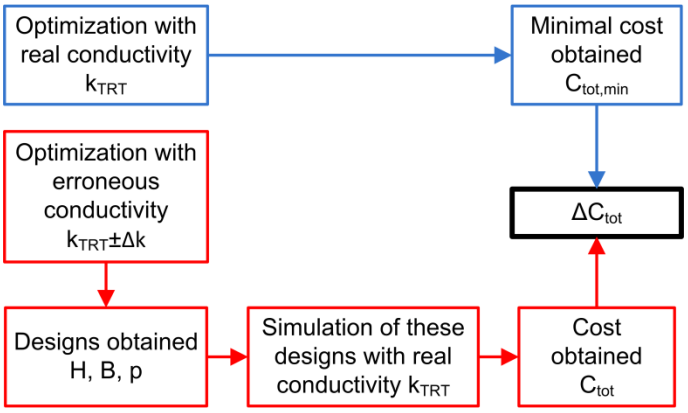
Optimization with real conductivity k_{TRT}
Minimal cost obtained $C_{tot,min}$
Optimization with erroneous conductivity $k_{TRT}\pm\Delta k$
ΔC_{tot}
Designs obtained H, B, p
Simulation of these designs with real conductivity k_{TRT}
Cost obtained C_{tot}

Figure 7

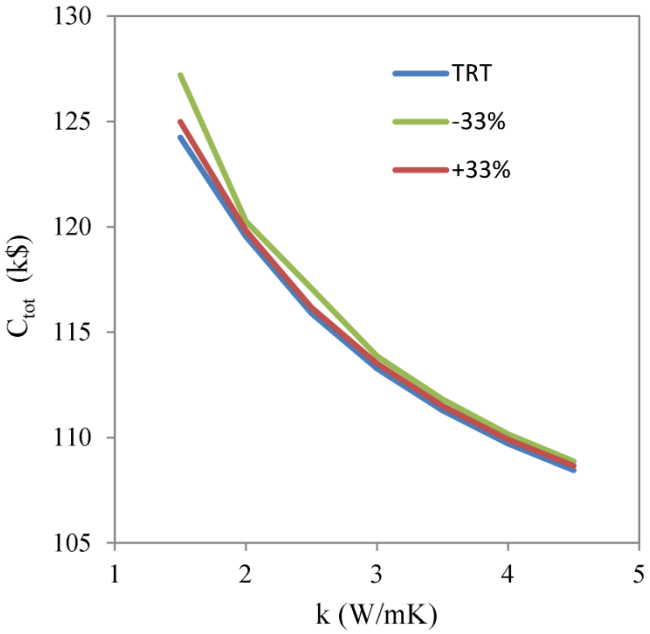

Figure 8

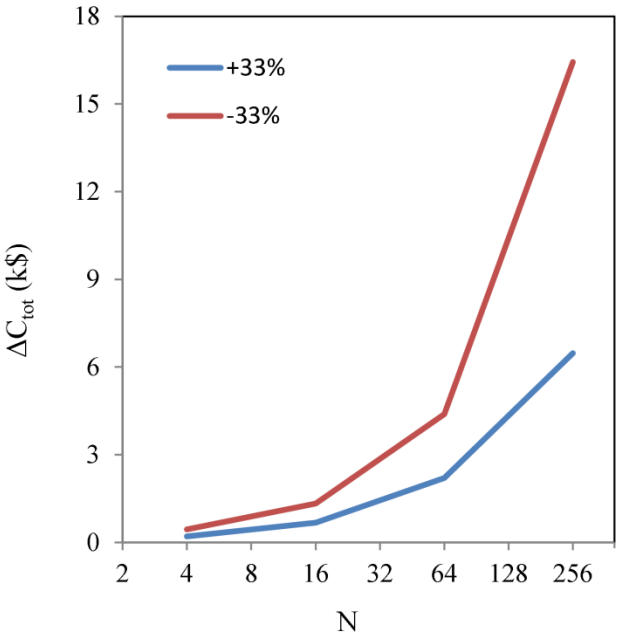

Figure 9

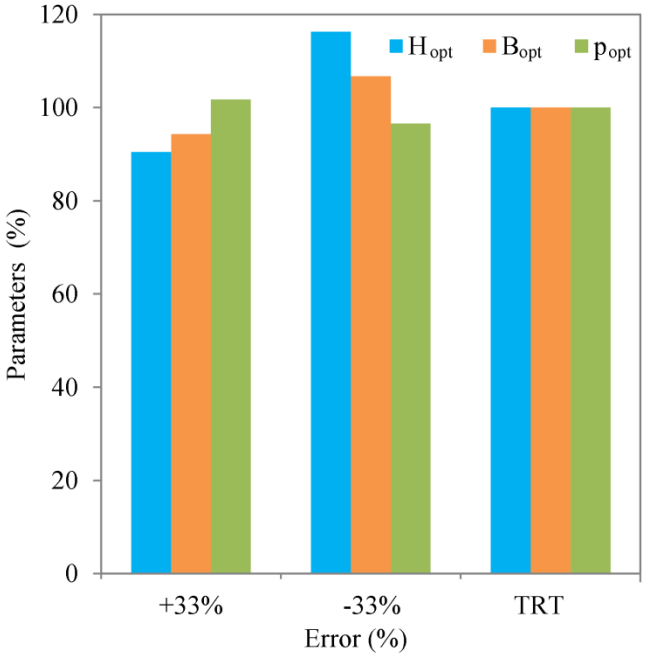

Figure 10

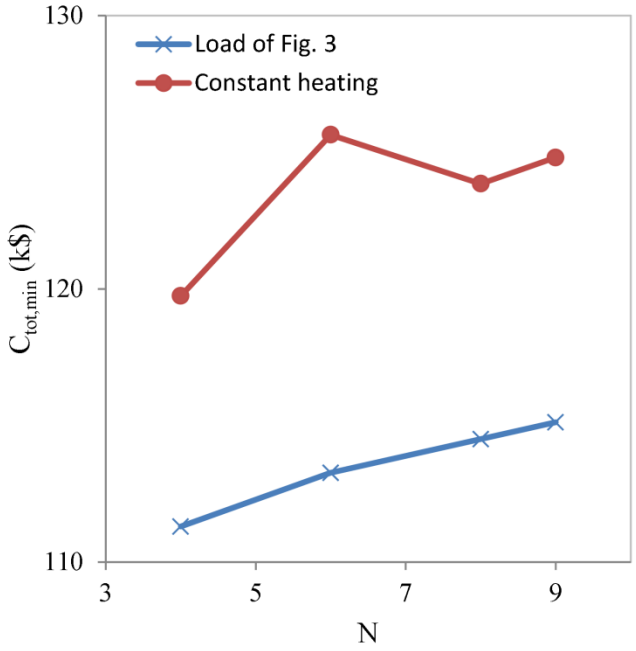

Figure 11

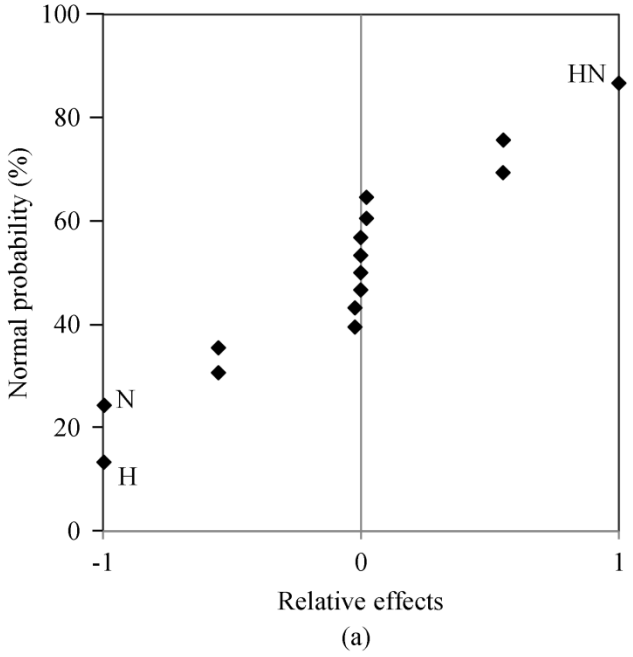
100
80
60
40
20
0
Normal probability (%)
HN
N
H
-1
0
1
Relative effects
(a)

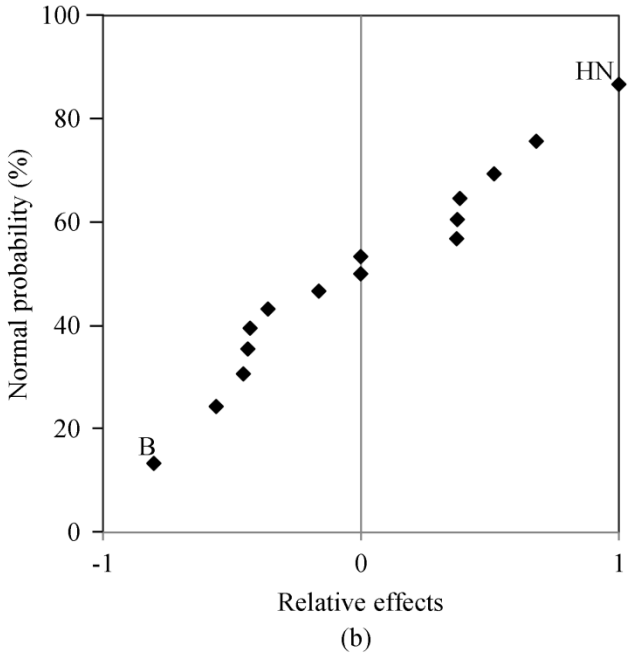
100
80
60
40
20
0
Normal probability (%)
HN
B
-1
0
1
Relative effects
(b)

Figure 12